Available online at www.sciencedirect.com
SCIENCE DIRECT®
Journal of Power Sources 127 (2004) 313–318
JOURNAL OF POWER SOURCES
www.elsevier.com/locate/jpowsour

Modelling and dynamic simulation of a fuel cell system with an autothermal gasoline reformer

Marc Sommer [a,*], Arnold Lamm [a], Andreas Docter [a], David Agar [b]

[a] *DaimlerChrysler, Research and Technology, Fuel Cell Systems, D-89013 Ulm, Germany*
[b] *University of Dortmund, Department of Chemical Engineering, Emil-Figge-Straße 66, D-44227 Dortmund, Germany*

Abstract

In order to describe the dynamic behaviour of a fuel cell system its components are modelled by the help of 1D dynamic models which are implemented in Matlab Simulink. The fuel cell system consists of an autothermal gasoline reformer (ATR) which for the realisation of a high system efficiency is thermally coupled to the other system components (gas purification, heat exchangers). Dynamic simulations of load changes show that the dynamic behaviour of such a system is primarily dominated by the response times of the liquid water flowing through the heat exchangers, the volume of which should consequently be reduced to a minimum in order to achieve shorter response times. In contrast, the dynamic behaviour of the reactors is not critical. The composition of the product gas at the ATR-outlet is however influenced by the moisture content of the gas at the ATR inlet, which in turn is negatively influenced for a short transition period by the residence times of the water flowing through the heat exchangers during a load change.

According to the results obtained, the system is able to adjust to load changes within 20 s for a load increase (10–90% of full load) and within 3 s for a load decrease (90–10% of full load).

Keywords: Fuel cell system; Dynamic simulation; Autothermal gasoline reformer; Modelling; Load change; Response time

1. Introduction

Fuel cell systems are considered to have a high potential to increase the efficiency of modern cars [1–3]. In order to make use of the existing infrastructure and to use the high-energy density of gasoline there's a lot of research going on in gasoline reforming for on-board hydrogen production in fuel cell vehicles [4–6].

To be an alternative to modern combustion engines, fuel cell systems with hydrogen production by gasoline reforming have to meet the following requirements:

- Fuel cell systems have to enable higher efficiencies than internal combustion engines in order to lower the fuel consumption of modern cars.
- The start-up time and the dynamic behaviour of such a vehicle has to be comparable to the one of modern cars.
- The emissions of a fuel cell vehicle have to meet the future emission regulations regarding CO, HC, NO_X and particles (e.g. SULEV, Euro V).
- They have to be competitive with regard to volume, weight and costs.

These requirements for fuel cell systems with on-board gasoline reformers are affected in particular by the operating parameters and the characteristics of the reformer whose efficiency is given by the heating value of the produced hydrogen in relation to the heating value of the fed gasoline:

$$\eta_{\text{Re former}} = \frac{\dot{n}_{H_2} \cdot \Delta H_{H_2}}{\dot{n}_{\text{Gasoline}} \cdot \Delta H_{\text{Gasoline}}}.$$

For the hydrogen production by gasoline reforming most publishers [7,8,4] prefer autothermal reforming concepts to steam reforming and partial oxidation because they enable

- a high hydrogen yield because of the addition of water to the feed;
- minimisation of NO_X− and soot-production by the addition of water and the low reaction temperatures (800–1000 °C);
- dynamic operation through in-situ-provision of the required energy because of exothermal reactions.

The operating parameters of autothermal reformers are the steam-to-carbon ratio S/C which brings the fed water into

* Corresponding author. Tel.: +49-731-5052982; fax: +49-731-5054211.
E-mail address: marc.sommer@daimlerchrysler.com (M. Sommer).

0378-7753/$ – see front matter © 2003 Elsevier B.V. All rights reserved.
doi:10.1016/j.jpowsour.2003.09.028

Nomenclature

a_v	specific catalyst surface area (m^2/m^3)
A	cross-section area of one channel (m^2)
$c_{p,g}$	heat capacity gas (J/mole K)
c_s	heat capacity solid (J/kg K)
$D_{i,g}$	diffusions coefficient of component i in the gas phase (mole/m s)
h	enthalpy of water (J/mole)
h'	enthalpy of liquid water at boiling point (J/mole)
$\dot{n}_C$	carbon mole flow (mole/s)
$\dot{n}_g$	gas mole flow (mole/s)
$\dot{n}_{Gasoline}$	gasoline mole flow (mole/s)
$\dot{n}_{H_2}$	hydrogen mole flow (mole/s)
$\dot{n}_{H_2O}$	water/steam mole flow (mole/s)
$\dot{n}_{O_2}$	oxygen mole flow (mole/s)
$\dot{n}_{O_2,stoich.}$	oxygen mole flow for stoichiometric combustion (mole/s)
R_j	reaction rate of reaction j (mole/m^2 s)
S/C	steam-to-carbon ratio
SR	stoichiometric ratio
T_g	gas temperature (K)
T_s	solid temperature (K)
u	velocity (m/s)
$\dot{V}_g$	gas flow rate (m^2/s)
$y_{i,g}$	mole fraction of component i in the gas phase
$y_{i,s}$	mole fraction of component i at the catalyst surface area
$\alpha_{s,g}$	heat transfer coefficient gas → solid (W/m^2 K)
β_i	mass transfer coefficient of component i (m/s)
Δh_b	enthalpy for vaporization (J/mole)
$\Delta H_{Gasoline}$	lower heating value of gasoline (J/mole)
ΔH_{H_2}	lower heating value of hydrogen (J/mole)
ΔH_j	enthalpy of reaction j (J/mole)
ε	porosity of catalyst structure
$\eta_{Reformer}$	reformer efficiency
λ_g	heat conductivity gas (W/m K)
λ_s	heat conductivity solid (W/m K)
$\nu_{i,j}$	stoichiometry coefficient of component i, reaction j
ρ_g	gas density (mole/m^2)
ρ_s	solid density (kg/m^2)

relationship with the carbon in the feed

$$S/C = \frac{\dot{n}_{H_2O}}{\dot{n}_C},$$

and the stoichiometric ratio SR which is defined as the amount of oxygen in the feed divided by the amount of oxygen necessary for complete combustion:

$$SR = \frac{\dot{n}_{O_2}}{\dot{n}_{O_2,stoich.}}.$$

In addition to these operating parameters, the reactor temperature of an autothermal reformer is influenced by the feed temperature.

In order to achieve high-system efficiencies, a suitable system configuration was developed with the help of the Pinch Point method and steady-state simulations (Aspen Plus), indicating a probable system efficiency of 30%. The fuel cell system, whose basic design is shown in Fig. 1 comprises the components ATR for the conversion of gasoline into hydrogen, high temperature shift reactor (HTS), low temperature shift reactor (LTS), preferential oxidation reactor (PrOX) for the gas purification, the fuel cell which produces electrical energy and the catalytic burner for the conversion of residual hydrogen together with the heat exchangers necessary for thermal coupling.

With respect to the above mentioned requirements there is also the need to optimise the dynamic behaviour of a fuel cell system based on gasoline reforming. The quicker the system is able to follow load changes the smaller, cheaper and less heavy is the necessary battery in the car.

For that purpose, the components of a fuel cell system with autothermal reformer have to be described by appropriate dynamic simulation models. These models have to be implemented in a simulation program which is able to solve differential equations with the help of a numeric solver. After implementation the dynamic reaction of the modelled fuel cell system on load changes from 10 to 90% of full load and from 90 to 10% of full load are calculated.

2. Development of dynamic models for the system components

The modelling of chemical reactors can be done in different ways of which the continuous models are the most important. Continuous models can be classified as homogeneous and heterogeneous models. Homogeneous models do not distinguish between the gas phase and the solid (catalyst) phase and therefore they have the advantage of a reduced number of numerical equations although this type of model is not suitable to locate Hot Spots in the catalyst phase [9]. In heterogeneous models, gas phase and catalyst phase are modelled separately and therefore they are able to describe the proceeding of a chemical reaction in detail and additionally they are able to localise and quantify Hot Spots. The disadvantage is the high number of numerical equations which may lead to numerical problems during the simulation [9].

Dynamic models for the system components are developed in the following manner:

- Because the reactions which occur in the water gas shift reactors are not very complex and their kinetics are known,

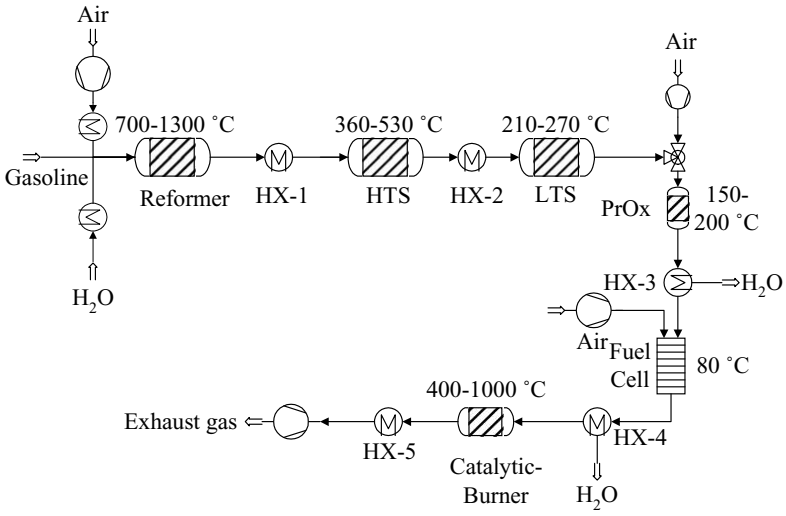

Fig. 1. Basic design of a fuel cell system with gasoline reformer.

these reactors are described by the help of heterogeneous models.

- The autothermal reactor is modelled by the help of a homogeneous model because the reactions occurring for which simplified kinetic data are available, are very complex.
- Considering the modelling of the other chemical reactors no reaction kinetic is available (PrOX, Catalytic Burner). In case of the fuel cell, the process description would require complex models. These components are described by the help of 1D dynamic models based on integral balances.
- The modelling of the heat exchangers is done by dynamic models which contain partial differential equations for the hot and the cold medium as well as for the heat transfer wall.

In the following, the modelling of a chemical reactor is described as an example for the water gas shift reactors.

The assumptions and simplifications made are:

- The pressure in the reactor is considered as constant.
- The gaseous phase is composed of H_2, CO, CO_2, N_2, H_2O and CH_4 and is with respect to the low pressure and the high temperature considered as ideal gas.
- The influence of radiation is neglected.
- The properties of the solid phase are considered as constant.
- The properties of the gaseous phase depend on composition, pressure and temperature and are described by the thermodynamic properties of the individual components in the ideal-gas state. The heat conductivity and the dynamic viscosity are approximated by the properties of N_2.
- The reactor is considered as an adiabatic device.
- The distribution of the gas on all channels of the monolith is ideal.
- There are no secondary reactions implemented.

Fig. 2 shows a balance element in a reactor where the catalyst is a solid phase and fixed on a monolithic carrier with many channels parallel to each other. The model considered is a dynamic, 1D model.

The following equations can be derived from the balances for energy and mass which are similar to those known from other authors e.g. [10]:

Energy balance for the gaseous phase:

$$\varepsilon\rho_{\mathrm{g}}c_{p,\mathrm{g}}\frac{\partial T_{\mathrm{g}}}{\partial t} = -\frac{1}{A}\frac{\partial}{\partial x}(\dot{n}_{\mathrm{g}}c_{p,\mathrm{g}}T_{\mathrm{g}}) + \varepsilon\lambda_{\mathrm{g}}\frac{\partial^2 T_{\mathrm{g}}}{\partial x^2} + \alpha_{s,\mathrm{g}}a_{\mathrm{v}}(T_{\mathrm{s}} - T_{\mathrm{g}})$$

Energy balance for the catalyst phase:

$$(1-\varepsilon)\rho_{\mathrm{s}}c_{\mathrm{s}}\frac{\partial T_{\mathrm{s}}}{\partial t} = (1-\varepsilon)\lambda_{\mathrm{s}}\frac{\partial^2 T_{\mathrm{s}}}{\partial x^2} - \alpha_{\mathrm{s,g}}a_{\mathrm{v}}(T_{\mathrm{s}} - T_{\mathrm{g}}) + (1-\varepsilon)\sum_j R_j\Delta H_j$$

Mass balances for the gaseous phase:

$$\varepsilon\rho_{\mathrm{g}}\frac{\partial y_{i,\mathrm{g}}}{\partial t} = -\frac{1}{A}\frac{\partial}{\partial x}(\dot{n}_{\mathrm{g}}y_{i,\mathrm{g}}) + \varepsilon D_{i,\mathrm{g}}\frac{\partial^2 y_{i,\mathrm{g}}}{\partial x^2} - \beta_i\rho_{\mathrm{g}}a_{\mathrm{v}}(y_{i,\mathrm{g}} - y_{i,\mathrm{s}})$$

$$\varepsilon\frac{\partial\dot{n}_{\mathrm{g}}}{\partial t} = -u\frac{\partial\dot{n}_{\mathrm{g}}}{\partial x} + a_{\mathrm{v}}\sum_j\left(\sum_i \nu_{i,j}\right)R_j$$

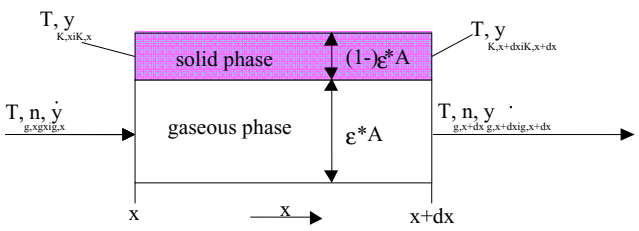

Fig. 2. Reactor element for the shift reactor models.

Mass balance for the catalyst phase:

$$(1-\varepsilon)\rho_g \frac{\partial y_{i,s}}{\partial t} = \beta_i \rho_g a_v (y_{i,g} - y_{i,s}) - (1-\varepsilon)\sum_j (\nu_{i,j} R_j)$$

As start conditions for $t = 0$ and $0 \le x \le L$ profiles for the variables in the reactor are implemented:

$$T_g(x,0) = T_g^0(x), \qquad T_s(x,0) = T_s^0(x),$$
$$y_{i,g}(x,0) = y_{i,g}^0(x) \qquad y_{i,s}(x,0) = y_{i,s}^0(x)$$

For the entrance of the reactor boundary conditions after Danckwerts [11] are implemented.

The kinetics for the water gas shift reaction are derived from experimental results and implemented in the reactor models.

The implementation of the reactor models in the simulation program Matlab Simulink is done a so-called S-function. The differential equations are solved with a numeric algorithm which is not able to solve partial differential equations. For that reason, a numerical solution of the partial differential equations is required. The numerical solution is done in the variable of space by the help of the method of finite differences.

3. Results and discussion

In the following, the results obtained for a thermally integrated system which is shown in Fig. 3 are presented. With the developed system models which are implemented in the simulation program Matlab Simulink load changes from 10 to 90% of full load and from 90 to 10% of full load are calculated. In this article, as an example the results for a load change from 10 to 90% of full load will be presented.

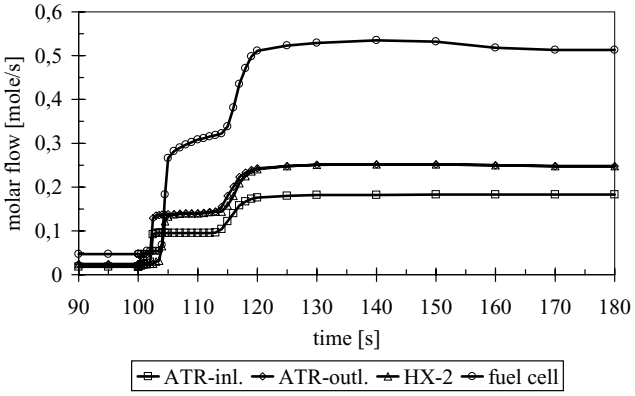

Fig. 4. Reformate flow at a load change from 10 to 90% of full load.

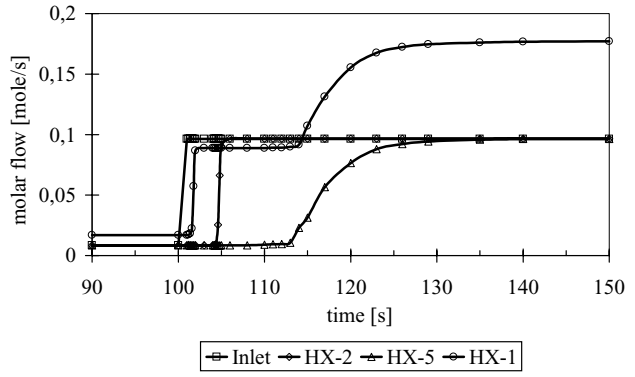

Fig. 5. Educt flow at a load change from 10 to 90% of full load.

Fig. 4 shows the reformate flow at a load change from 10 to 90% of full load. The new steady-state after the fuel cell is reached after approximately 20 s. The reason for this behaviour is made clear by Fig. 5 which shows the educt flow at this load change. The educt flow at the outlet of

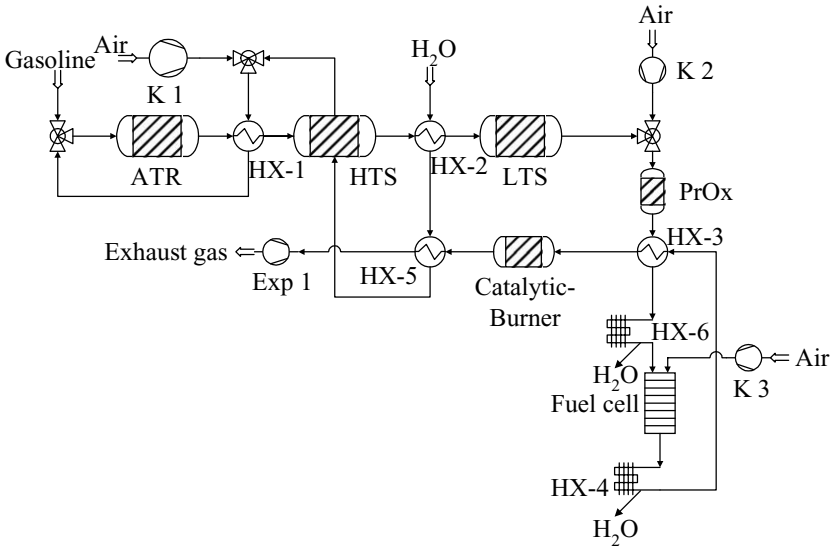

Fig. 3. Thermally integrated system used in the calculations of load changes.

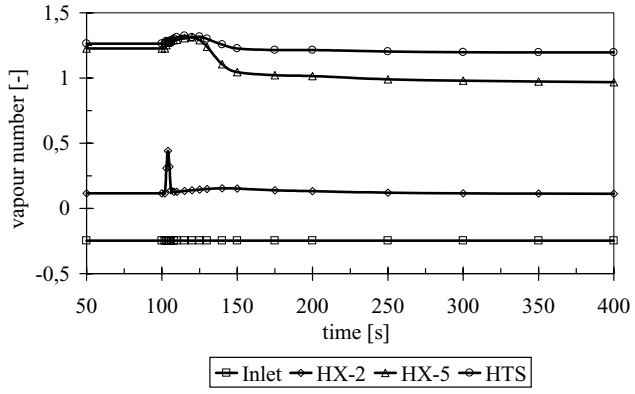

Fig. 6. Vapour number at a load change from 10 to 90% of full load.

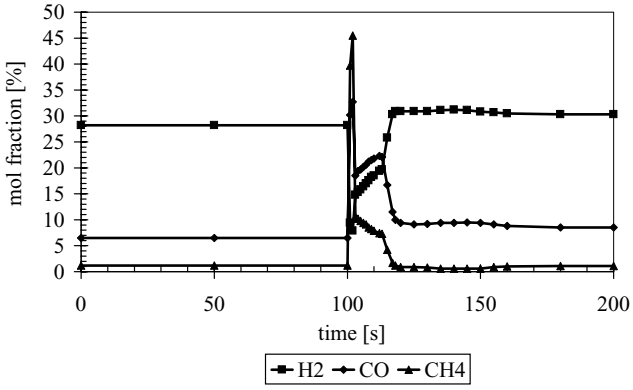

Fig. 8. Reformate composition at ATR-outlet at a load change from 10 to 90% of full load.

the heat exchanger HX-1 rises for the first time when the higher air flow out of the compressor K-1 has flown through HX-1. The response time of the educt flow is dominated by the residence time for the demanded water in the heat exchangers, which is mainly influenced by heat exchanger HX-5 which is a large heat exchanger and heat exchanger HX-2 where the water is nearly not vaporised. So also the reformate flow is influenced by the educt flow and shows a similar behaviour.

Fig. 6 shows the vapour number of the educt flow (water) at the load change. The vapour number is defined as water enthalpy standardised on the state of boiling:

$$\text{vapour number} = \frac{h - h'}{\Delta h_b}.$$

The educt water is fully vaporised after it has flown through the heat exchanger HX-5. In the heat exchanger HX-2, it is nearly liquid and this causes a high residence time because of the high density. The vapour number reaches its steady-state after approximately 50 s.

Fig. 7 shows the educt temperature at the outlet of heat exchanger HX-1 and the inlet of the ATR and the reformate temperature at the ATR outlet. The temperature of educt at the outlet of the heat exchanger HX-1 only shows a slight and soft increase. The temperature of educt at the ATR inlet is influenced by the different residence times for air and water in the system. At a load change from 10 to 90% of full load gasoline is mixed with a lower stream of air and water which causes a decrease in temperature. It reaches steady-state after 25 s when the flow of air and water has reached their normal level. In consequence, the operation parameters for the ATR are temporarily shifted to abnormal conditions (very low S/C, normal SR). This is the reason for the increase of the ATR outlet temperature in the range of 100 K. In addition, temperature peaks especially at the catalyst front where partial oxidation of gasoline is the main reaction are possible.

The consequences on the product composition at the ATR outlet are shown in Fig. 8. The mole fractions for CH_4 and CO increase, whereas the H_2 mole fraction decreases. The short peak for CH_4-mole fraction is a consequence of the low SR in the first 2 s after the load change. Because of the low S/C in the first 20 s after the load change the water gas shift reaction in the ATR is obstructed and consequently less CO is converted into H_2. A normal product composition is reached after 25 s when the operating parameters have reached the demanded conditions.

Fig. 9 shows the temperature and the CO concentration in the shift reactors at a load change from 10 to 90% of

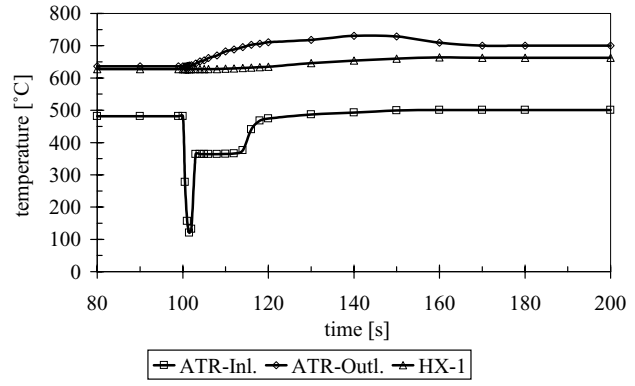

Fig. 7. Temperature at HX-1-outlet, ATR-inlet and ATR-outlet at a load change from 10 to 90% of full load.

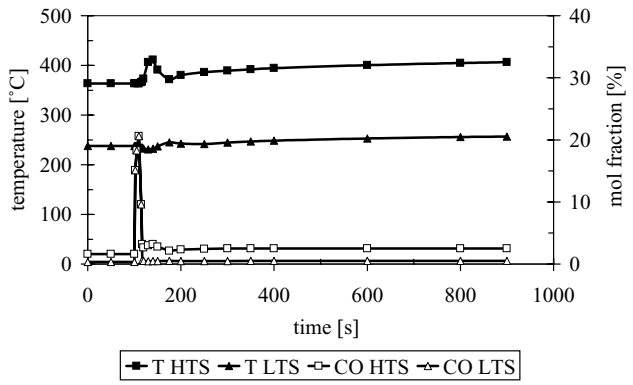

Fig. 9. Shift-reactor temperature and CO-concentration at a load change from 10 to 90% of full load.

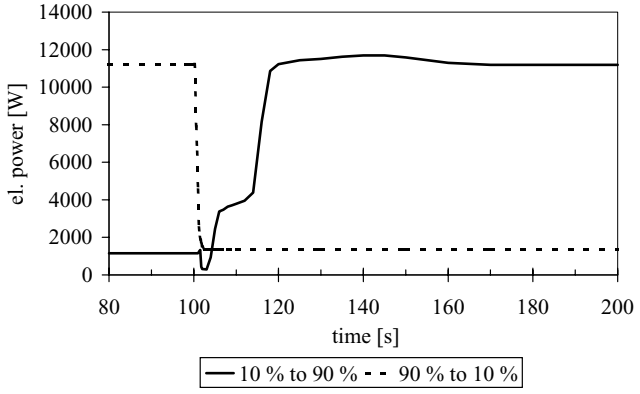

Fig. 10. Electrical power from fuel cell at a load change from 10 to 90% and from 90 to 10% of full load.

full load. The temperatures of the shift reactors are mainly influenced by the performance and the thermal mass of the heat exchangers placed in front of them (HX-1/HX-2). For that reason, they reach steady-state after approximately 300 s. Because of the lack of water in the heat exchanger HX-1 during the first 20 s the reformate cannot be cooled down so far as foreseen in the design state, consequently the temperature of the HTS rises. In the heat exchanger HX-2, the whole amount of water is available immediately, the reformate is cooled too strongly. The temperature in the LTS decreases. Due to the high CO production in the ATR also the CO concentration at the outlet of the shift reactors is much higher than in the design state. Steady-state for the CO concentrations in these reactors is reached after nearly 100 s.

Fig. 10 shows the electrical power available from the fuel cell for the two load changes. The electrical power available from the fuel cell depends on the reformate mole-flow and the H_2 concentration. For a load change from 10 to 90%, it reaches steady-state after 20 s, for a load change from 90 to 10% it is reached after 3 s. The curves for the reformate mole flow are reflected. The curve for the load change from 10 to 90% also reflects the decrease of H_2 concentration due to the too low SR and S/C in the ATR.

The results for a load change from 90 to 10% of full load are based on the same effects, but the response times are longer because of the lower gas flows.

4. Conclusion

According to the results obtained the dynamic behaviour of the reformer is mainly influenced by the volume of the different components which has an influence on the residence times. The calculations also show that the dynamic behaviour is also influenced by the mass of each component whose high heat capacity on the one hand leads to a function as an energy storage and on the other hand absorbs changes in temperature with the result that it takes much longer for the temperature to reach the new steady-state but also prevents the component from temperature peaks as it works like a buffer.

In order to make the reformer as dynamic as possible one has to construct a compact and light-weight reactor system which enables short residence times of the gases in the different sections and short times for the temperature to reach its new steady-state.

The calculated response times also show that even in regard of the action items described in order to construct a dynamic reformer the dynamic behaviour of the system will be too slow to work as a propulsion system without any energy storage. The required system dynamic for mobile applications is a response time of 1 s for a load change from 10 to 90% of full load. So it can be easily estimated that the required dynamic of such a system will only be achieved with the help of a battery which is electrically loaded by the fuel cell system. Nevertheless it is absolutely necessary to build a fuel cell system which is as dynamic as possible because with increasing dynamic of the fuel cell system the required capacity and power of the battery becomes lower and the battery itself becomes cheaper and lighter.

Acknowledgements

The work described in this article was supported by a grant of the German “Bundesministerium für Bildung und Forschung”.

References

[1] R. Krüger, A. Voß, Systemanalytischer Vergleich inovativer Kraftstoffe und Antriebssysteme. VDI-Berichte 1565 (2000) 493–528.
[2] T. Dreier, P. Tzscheutschler, Ganzheitliche Betrachtung innovativer Fahrzeugantriebe und alternativer Kraftstoffe. VDI-Berichte 1565 (2000) 555–569.
[3] M. Pehnt, J. Nitsch, Ökobilanzen und Markteintritt von Brennstoffzellen im mobilen Einsatz. VDI-Berichte 1565 (2000) 323–347.
[4] A. Docter, A. Lamm, Gasoline fuel cell systems, J. Power Sources 84 (1999) 194–200.
[5] S. Ahmed, M. Krumpelt, Hydrogen from hydrocarbon fuels for fuel cells, Int. J. Hydrogen Energy 26 (2001) 291–301.
[6] W.L. Mitchell, J.C. Cross, J.M. Bentley, Development of multi-fuel hybrid partial oxidation fuel processors for fuel cell vehicles and hydrogen re-fueling stations, in: Proceedings of the 30th Annual ISATA Conference, Florence, 1997.
[7] R. Kumar, S. Ahmed, M. Krumpelt, K.M. Myles, Improved fuel cell system for transportation applications, US Patent 5,248,566 (1993).
[8] T.S. Christensen, I.I. Primdahl, Improve syngas production using autothermal reforming. Hydrocarbon Process. 1994 (1994) 39–46.
[9] R. Adler, Stand der Simulation von heterogen-gaskatalytischen Reaktionsabläufen in Festbettrohrreaktoren—Teil 1, Chem. Ing. Tech. 72 (2000) 555–564.
[10] S. Feyo De Azevedo, M.A. Romero-Ogawa, A.P. Wardle, Modelling of tubular fixed-bed catalytic reactors: a brief review, Trans. IChem. E. 68 (1990) 483–502.
[11] P.V. Danckwerts, Continuous flow systems, Chem. Ing. Sci. 2 (1953) 1–13.